Atmos. Chem. Phys. Discuss., 9, 13569–13592, 2009
www.atmos-chem-phys-discuss.net/9/13569/2009/

Atmospheric Chemistry and Physics Discussions

This discussion paper is/has been under review for the journal *Atmospheric Chemistry and Physics (ACP)*. Please refer to the corresponding final paper in *ACP* if available.

UV aerosol indices from SCIAMACHY: introducing the SCattering Index (SCI)

M. Penning de Vries, S. Beirle, and T. Wagner

Max Planck Institute for Chemistry, J.-J.-Becherweg 27, 55128 Mainz, Germany

Received: 27 April 2009 – Accepted: 11 June 2009 – Published: 19 June 2009

Correspondence to: M. Penning de Vries (marloes@mpch-mainz.mpg.de)

Published by Copernicus Publications on behalf of the European Geosciences Union.

Abstract

The Absorbing Aerosol Index (AAI) is a useful tool for detecting aerosols that absorb UV radiation – especially in cases where other aerosol retrievals fail, such as over bright surfaces (e.g. desert) and in the presence of clouds. The AAI does not, however, consider contributions from "scattering" (hardly absorbing) aerosols and clouds: they cause negative AAI values and are usually discarded. In this paper, we demonstrate the use of the AAI's negative counterpart, the SCattering Index (SCI) to detect "scattering" aerosols. Maps of seasonally averaged SCI show significantly enhanced values in summer in Southeast USA and Southeast Asia, pointing to high production of "scattering" aerosols (presumably mainly sulphate aerosols and organic aerosols) in this season. The application of a cloud filter makes the presence of "scattering" aerosols even more clear. In a comparison of AOT from AERONET and our Aerosol Indices from SCIAMACHY, good agreement was found for two AERONET stations in Southeast USA, and two stations in Africa. This fact confirms the suitability of SCI as a tool to detect "scattering" aerosols.

The combination of the UV Aerosol Indices AAI and SCI provides the unique possibility to characterise absorbing properties of aerosols from space. Accurate knowledge about aerosol absorption is crucial for the correct determination of the contribution of aerosols to the radiative budget.

1 Introduction

Due to the large variety of sources, aerosol particles have strongly varying microphysical properties. As a consequence, aerosol optical properties (aerosol optical thickness (AOT), single scattering albedo (ω_0), and phase function), and their respective wavelength dependences can differ markedly for different aerosol types. This issue causes difficulties for the retrieval of aerosol parameters by passive satellite instruments. Another important complicating factor is the existence of an aerosol particle size distri-

ACPD

9, 13569–13592, 2009

bution, rather than a single unique particle size: this causes a smooth, wavelength-dependent effect on remotely sensed optical spectra that is difficult to distinguish from changes in wavelength-dependent surface albedo. Also, aerosol parameters are usually not retrieved in the presence of clouds, meaning that many measurement points are discarded, and that results averaged over certain time scales are biased towards cloudless scenarios.

Some thirteen years ago, a "new absorbing aerosol index" was introduced (Hsu et al., 1996) that was found to be very sensitive to UV-absorbing aerosols. This aerosol index is based on the measurement of the reflectance at two wavelengths in the UV coupled with radiative transfer modelling of the Rayleigh atmosphere. It was developed for TOMS, but in later years was adapted for use with GOME (Gleason et al., 1998; de Graaf et al., 2005), SCIAMACHY (de Graaf et al., 2005b), and OMI (Torres et al., 2007). The Absorbing Aerosol Index (AAI) has proven to be very useful for studying UV-absorbing aerosols such as biomass burning aerosols (e.g. Hsu et al., 1996, 2003; Herman et al., 1997; Gleason et al., 1998; Fromm et al., 2005; Fromm et al., 2006; de Graaf et al., 2006) and desert dust (e.g. Herman et al., 1997; Chiapello et al., 1999; Mahowald and Dufresne, 2004; Darmenova et al., 2005; de Graaf et al., 2006). This is despite the fact that quantitative information on aerosol optical thickness or single scattering albedo is hard to obtain due to the strong height dependence of AAI (Herman et al., 1997; Hsu et al., 1999; Mahowald and Dufresne, 2004). Three reasons that make AAI such a useful quantity are (1) that it is not very sensitive to surface type, which allows retrieval over land (even desert) and water alike using the same algorithm. Also, (2) the AAI can be retrieved in the presence of clouds, and is in fact even more susceptible to absorbing aerosols above strongly reflective surfaces (clouds, snow, ice) (Torres et al., 1998; Hsu et al., 2003; de Graaf et al., 2006). And (3), the Aerosol Indices contain information about aerosol layer height.

In this paper, we introduce the UV SCattering Index (SCI). Like its counterpart, the AAI, it is an indicator for the presence of aerosols, in this case "scattering" aerosols (meaning aerosol particles with weak absorption in the UV range), and clouds. To the

ACPD
9, 13569–13592, 2009

authors' knowledge, no detailed investigations on the SCI have been performed so far, presumably because the effects of clouds make the SCI difficult to interpret.

We chose to use the SCIAMACHY instrument for this study because it has a lot of potential for characterizing aerosols in detail. The instrument detects a large wavelength range from the UV and the visible range to the near-IR. SCIAMACHY spectra are mainly used for trace gas analysis using the DOAS method (Platt, 1994; Bovensmann et al., 1999; Wagner et al., 2008). SCIAMACHY offers the possibility to detect aerosol effects on radiance at many different wavelengths, in addition to providing information from trace gas absorption features that are also affected by the presence of aerosols (e.g. O_2 or O_4, see Koelemeijer et al., 2001; Wagner et al., 2004; van Diedenhoven et al., 2005). Such a large number of independent measurements may be of use for the accurate retrieval of aerosol optical properties in the near future. Another important advantage of the large wavelength range of SCIAMACHY is that aerosol properties can be studied at UV and visible wavelengths, where their signal is usually strongest, whereas clouds can be detected at visible to near-IR wavelengths, where the influence of aerosols is much weaker.

The paper is structured as follows: in the following two sections, we give a short explanation of the method and demonstrate the sensitivity of AAI and SCI to different (aerosol) parameters. In Sect. 4 we present our recent UV Aerosol Index results, and the effect of a cloud filter on these results is illustrated in Sect. 5. Our data are subsequently compared to AERONET ground-based sun photometer measurements (Holben et al., 1998). Section 7 describes the effects of clouds on Aerosol Indices in some detail, and the main conclusions of the paper are summarized in Sect. 8.

2 Method

The AAI is derived from the so-called residue (r_λ) (Torres et al., 1998). This residue is essentially a measure of the change in the amount of Rayleigh scattered light observed at the top of atmosphere caused by the presence of aerosols (or optically thin

ACPD
9, 13569–13592, 2009

and partial clouds). The r_λ is calculated using reflectances at two wavelengths in the UV range, λ and λ_0. We selected λ=335.5 nm and λ_0=376.5 nm, because at these wavelengths the reflectance is not strongly influenced by O_3 and other trace gas absorption or Fraunhofer lines. The wavelengths also lie outside of the range of a broad spectral feature around 360 nm that is caused by an error in SCIAMACHY's radiometric calibration.

In analogy to r_{340} from TOMS in Torres et al. (1998), our r_{335} is calculated using the reflectance measured at 335.5 nm (R^{meas}), and that calculated at the same wavelength for a model atmosphere devoid of aerosol (R^{Rayl}). The surface albedo for the calculation of R^{Rayl} is derived from the measured reflectance at 376.5 nm. The r_{335} is defined as (Torres et al., 1998):

$$r_{335} = -100 \cdot^{10} \log \left(\frac{R^{\text{meas}}}{R^{\text{Rayl}}} \right)_{335.5} \quad (1)$$

For the calculation of r_{335}, look-up tables (LUTs) were constructed that contain reflectances at λ and λ_0 for a Rayleigh atmosphere with six surface albedo values between 0 and 1. The LUTs were modelled using the radiative transfer model (RTM) SCIATRAN 3.0, a successor to SCIATRAN 2.0 (Rozanov et al., 2002, 2005) (downloaded from: http://www.iup.physik.uni-bremen.de/sciatran/downloads/). Reflectances were calculated using the vector discrete ordinate method in a plane-parallel atmosphere, taking polarisation into account. In earlier tests, it was found that including polarisation is critical to the correct calculation of r_{335} (not shown, but see de Graaf et al., 2005b).

In brief, the algorithm functions as follows. For each SCIAMACHY ground pixel reflectances at λ and λ_0 are read out. The relevant look-up-table (LUT) is then selected from a library based on the solar zenith angle (SZA), on the viewing geometry (given by the line-of-sight zenith angle, the line-of-sight azimuth angle, and the solar azimuth angle), and on the average altitude of the ground pixel (determined by averaging of the GTOPO 0.1°×0.1° altitude world map [http://edc.usgs.gov/products/elevation/gtopo30/

ACPD
9, 13569–13592, 2009

gtopo30.html]). Using the measured reflectance at 376.5 nm, the matching Rayleigh reflectance at 335.5 nm is determined from the selected LUT. The measured reflectance and the "looked up" Rayleigh reflectance at 335.5 nm are inserted into Eq. (1) to obtain r_{335}.

The positive part of r_{335} is commonly defined as the Absorbing Aerosol Index (AAI); we define the negative part of r_{335} as the new SCattering Index (SCI):

$$\text{AAI} = r_{335} \text{ for } r_{335} \geq 0, \text{ undefined for } r_{335} < 0 \quad (2)$$

$$\text{SCI} = -r_{335} \text{ for } r_{335} \leq 0, \text{ undefined for } r_{335} > 0 \quad (3)$$

In the following pages, the term "UV Aerosol Indices" (UVAI) will be used for the combination of AAI and SCI.

3 Sensitivity of UVAI

The subject of sensitivity of UVAI to various parameters has been addressed in several model studies. Herman and co-workers found a near-linear dependence of UVAI on aerosol optical thickness (AOT), and an equally strong dependence on aerosol layer altitude (Herman et al., 1997; Hsu et al., 1999; Mahowald and Dufresne, 2004). Of the other aerosol optical parameters, the single-scattering albedo (ω_0) has the largest influence on UVAI, especially if ω_0 is wavelength-dependent in the UV range (Torres et al., 1998; de Graaf et al., 2005). We have modelled UVAI for many different aerosol scenarios using the RTM SCIATRAN 3.0, and have found similar results as reported previously in Torres et al. (1998); de Graaf et al. (2005). Some of the results are summarized in Fig. 1. The dependence of UVAI on ω_0 is shown for two values of AOT for an aerosol with an Ångström coefficient of 1.5. The modelled AOT profile is triangle-shaped, has a total geometrical thickness of 2 km, and has a maximum AOT at 2, 4, or 6 km altitude as shown in the figure legend.

In addition to their dependence on aerosol parameters, UVAI are sensitive to the scattering angle (i.e., solar zenith angle and viewing geometry (de Graaf et al., 2005)),

ACPD
9, 13569–13592, 2009

and very slightly to surface albedo (Torres et al., 1998; de Graaf et al., 2005). Although UVAI are sensitive to the ozone total column, the effect is small (UVAI increase by 1 unit for a change from 100 DU to 500 DU for the 340/380 nm wavelength pair (de Graaf et al., 2005)), and is currently not taken into account in our algorithm.

As mentioned above, it was shown that neglect of polarisation in the calculation of r_λ can lead to large errors, especially when the relative azimuth angle <90° (de Graaf et al., 2005b). Polarisation is of importance for radiative transfer modelling in the UV range because of the rather large number of polarizing Rayleigh scattering events (Mishchenko et al., 1994) (on average approximately 2 at λ=335.5 nm for clear sky, and this number increases with increasing surface reflectivity).

4 Seasonal averages of UVAI

In Fig. 2, we show results from our UVAI algorithm: seasonally averaged UVAI for the months January to March and for July to September 2005. The colour scale was chosen to make absorbing aerosols appear in blue, scattering aerosols and clouds in yellow and red. No cloud filtering was applied to obtain these figures, but pixels in sun glint geometry (sun glint deviation angle <18°, see Tilstra, 2008) were discarded. We also removed pixels where solar zenith angle (SZA) is greater than 60°, because for higher SZA the UVAI become increasingly dependent on solar and viewing angles (see Fig. 1 in de Graaf et al., 2005). Due to the wavelength-dependent degradation of SCIAMACHY the UVAI have been drifting to ever higher values since the end of 2004 (Tilstra et al., 2007). This drift is so substantial that data of the three months in 2005 shown in Fig. 2 may not be simply summed, but rather need to be corrected using a time-dependent offset. The offset was chosen so that the average UVAI determined for cloudy pixels (cloud fraction >90%) in a control region in the northern Pacific ocean was near zero (see Sect. 7) over the whole year (not shown).

The most important sources of UV-absorbing aerosols are biomass burning and deserts. In most of the so-called global dust belt (the world's largest deserts in Africa

ACPD
9, 13569–13592, 2009

and Asia between 20°–40° N) the meteorological situation is most favourable for desert dust formation in the months July, August and September, causing the largest AAI values in that season. Biomass burning activity also depends on season: in December and January, many fires are found in sub-Saharan Africa, whereas in February and March, large-scale agricultural burning takes place in Southeast Asia. On the Southern Hemisphere, most notably in the Amazon rainforest and in southern Africa, the biomass burning season peaks in August and September. The AAI results shown in Fig. 2 are very similar to previously shown results from GOME and SCIAMACHY (de Graaf et al., 2005a, b; http://www.temis.nl/airpollution/absaai/), and from OMI (http://toms.gsfc.nasa.gov/aerosols/aerosols_v8.html).

The SCI results have not been shown in this fashion before. In Fig. 2, there are some apparent hotspots concerning the SCI: in the Amazon, Northwest Mexico, and Indonesia (both plots), in southern Africa (upper plot), and in central Africa, Southeast USA, and Southeast Asia (lower plot). Although clouds can make a significant contribution to the SCI (as discussed in detail below), we will provide evidence that these "hotspots" are most probably not – or not completely – caused by cloud cover.

5 Cloud filter

To eliminate cloud effects, we filtered the data shown in Fig. 2 by removing ground pixels containing cloud fractions higher than 5% according to the HICRU algorithm (Grzegorski et al., 2006). The results are shown in Fig. 3. The threshold value of 5% was chosen to remove most of the cloudy pixels without losing pixels containing aerosols misclassified as clouds. Geometrically small and optically thin (e.g. cirrus) clouds could escape the cloud filtering procedure, and are expected to contribute to the UVAI signal; this topic will be considered in more detail in Sect. 7 of this paper.

In comparing Figs. 2 and 3, the effect of clouds on UVAI (mainly SCI) immediately becomes clear. Whereas in Fig. 2 the oceans are almost completely coloured yellow (SCI is around 1), in Fig. 3 a more grey background is seen, indicating a value much

ACPD
9, 13569–13592, 2009

closer to 0 for most of the oceans. The patterns of the absorbing aerosols remain the same after cloud-filtering of the data, although some pixels containing mineral dust over ocean have apparently been mistaken for clouds and have therefore been discarded. Also, in the lower figure most of the biomass burning plumes in the Amazon and especially in southern Africa have disappeared after cloud-filtering. The reason is that in these regions, absorbing aerosols often co-exist with clouds, in some cases forming an aerosol layer above low-lying clouds (see e.g., de Graaf et al., 2006; Chand et al., 2008). These pixels are discarded as a consequence of our cloud-filtering procedure.

The "SCI hotspots" mentioned in the previous section have remained after cloud-filtering. These high SCI signals have two main origins: aerosols with high ω_0 (at least in the UV range, hereafter designated as "scattering" aerosols); or persistent cirrus and other thin or fractional clouds that have slipped through the cloud filter. The contribution of clouds to SCI is still significant in Fig. 3, e.g., over large parts of the oceans (although part of this signal probably comes from "scattering" aerosols). Nevertheless, the spatial patterns of several areas with high SCI (most notably Northwest Mexico, Southeast USA and Southeast Asia) appear to be in agreement with the presence of "scattering" aerosols. In addition, the average SCI values in these and other regions are much higher than would be expected from clouded scenes alone (as will be shown in Sect. 7).

6 Comparison of UVAI with AOT from AERONET

The hypothesis that SCI in Southeast USA is not (or not predominantly) caused by the presence of clouds is backed by the good agreement between UVAI and AOT data from AERONET ground-based sun photometer measurements at two stations in the Southeast USA, shown in Fig. 4. For the comparison of AERONET AOT with UVAI of absorbing aerosols, measurements from two stations in Africa are shown in Fig. 5.

For the UVAI averages, a region of four square degrees around each AERONET station was selected, and UVAI data were averaged for the selected region either on a daily or a monthly basis. Measurements where the HICRU cloud fraction exceeded

ACPD
9, 13569–13592, 2009

5% were discarded, as were measurements where SZA exceeded 60°. The data from AERONET are both daily and monthly averaged AOT data, measured at 340 nm. AOT data are cloud-cleared level 2.0 data, although level 1.5 data were included in the figure for Walker Branch (orange line) for the lack of level 2.0 AOT data in the first five months of 2005. AERONET measurements with SZA >60° were discarded, and only those data points are displayed that were measured between 9 a.m. and 11 a.m. (local time) to better match the satellite overpass time (10 a.m. local time at the equator).

In the lower panels in Figs. 4 and 5, the AERONET level-1.5 single-scattering albedo values determined at 440 nm are shown. The value of ω_0 depends on wavelength (Dubovik et al., 2002), with ω_0 at 440 nm usually smaller than in the UV range. However, some aerosols are more absorbing in the UV range, for example in the case of mineral dust or "brown" carbon aerosols (Dubovik et al., 2002; Kirchstetter et al., 2004; Barnard et al., 2008). For the examples shown in Figs. 4 and 5, ω_0 at 440 nm appears to be a good indicator of absorbing (ω_0 roughly below 0.9) and "scattering" (ω_0 roughly above 0.9) aerosols: high SCI values correspond to days with high AOT and high ω_0, whereas high AAI values correspond to days with high AOT and low ω_0.

For the two stations in Southeast USA, the monthly averaged UVAI is significantly anti-correlated with monthly averaged AERONET measurements of AOT at 340 nm (Fig. 4; R^2=0.74 and R^2=0.64 for monthly averages at Walker Branch and GSFC AERONET stations, respectively). The reason for this anti-correlation of UVAI, meaning a positive correlation with SCI, is the presence of "scattering" aerosols. In the plots with single scattering albedo it can be seen that for the season with high AOT, the aerosols are highly reflective (ω_0 at 440 nm is between 0.95 and 1.0). This is in agreement with the hypothesis that the aerosols detected at GSFC and Walker Branch stations are mainly secondary organic aerosols formed by reactions of volatile organic compounds with atmospheric trace gases, such as NO_x and SO_x (Goldstein et al., 2009).

For the two AERONET stations in Africa, Ilorin and Mongu, the correlation between AOT and UVAI is positive (Fig. 5; R^2=0.43 and R^2=0.96 for monthly averages at Ilorin and Mongu AERONET stations, respectively). AOTs are very high in the biomass

ACPD
9, 13569–13592, 2009

burning seasons (December–March in Ilorin, July–October in Mongu), and the large AAI values indicate that the aerosols form high-level dark aerosol plumes: low-level aerosol layers would cause much smaller – or even negative – UVAI values (see Fig. 1). In the biomass burning season at Mongu, the number of cloud-cleared AERONET measurements decreases sharply, probably because of increased cloud formation due to aerosol particles. Nevertheless, the onset of the biomass burning season can be seen in the upwards trends in AOT and aerosol absorption (decreasing ω_0) in June and July. At Ilorin, the number of AERONET measurements decreases outside of the biomass burning season due to persistent cloud cover, as is reflected by the number of data points included in the monthly averaged AOT, visualized by the size of the data points in Fig. 5. The number of data points in the UVAI plot decreases sharply when only pixels with CF <5% are included, instead of a less strict CF threshold of, e.g., 10%. Scenes with heavy aerosol loading may in this case have been misclassified as "cloudy" by the HICRU algorithm. This remains to be investigated.

7 Cloud modelling

The SCI can be retrieved in presence of clouds, but it is also strongly influenced by them, especially by geometrically small or optically thin clouds. In Fig. 6 the results of a cloud sensitivity study are shown, in which clouds were modelled with either a fixed optical thickness of 50 and varying geometrical CF, or with varying optical thickness and fixed geometrical CF equal to 1. The resulting UVAI depends strongly on effective CF, and is systematically different for optically thin (geometrical CF=1) and optically thick (optical thickness=50) clouds. The most important results from the cloud-modelling study are: 1. partial and thin clouds cause negative UVAI (non-zero SCI); 2. clouds with effective CF between 5% and 50% cause the largest SCI, and 3. the height of the clouds has a minor influence on the SCI (cf. Fig. 1).

From the right plot in Fig. 6 it follows that a cloud filter with a CF threshold of 5% does not exclude the effect of small clouds to the UVAI signal completely. This has an effect

on SCI, but also on AAI, especially when temporal or spatial averages are observed: small negative UVAI caused by clouds cause a decrease in the average UVAI value. Because the simple cloud fraction threshold is not an adequate filter for small and thin clouds, we are working on an improved cloud correction method for the UVAI that exploits the differences in wavelength dependence of cloud and aerosol optical parameters (most notably, optical thickness). The cloud correction will be beneficial to both SCI and AAI, because thin clouds reduce the AAI in the same way as they enhance the SCI.

8 Conclusions

In this paper we introduced the SCI as an indicator for the presence of "scattering" aerosols (that barely absorb UV radiation) and thin or partial clouds. The SCI is a counterpart to the more generally known AAI, which has been used for over a decade as a semi-quantitative measure of aerosols that absorb UV radiation. Advantages of AAI include the insensitivity to surface type and the possibility to calculate AAI in the presence of clouds. For the SCI, the same advantages apply, making it a useful tool for the monitoring of "scattering" aerosols. We note here, however, that for the correct interpretation of SCI and AAI clouds have to be taken into account.

The SCI, averaged over a suitable time range, can nevertheless be used to study "scattering" aerosols. The global distribution of SCI (Figs. 2 and 3), its seasonal cycle, and the high seasonally averaged SCI values in some regions are indications that "scattering" aerosols (and not only clouds) are being detected. The significant correlation between monthly averaged SCI and AOT (Fig. 4) at the GSFC and Walker Branch AERONET stations are a good argument that SCI is, indeed, an indicator of "scattering" aerosols.

With the UV Aerosol Indices, AAI and SCI, we have a unique tool for the direct detection of the absorptive properties of aerosols from space: no assumptions on aerosol optical parameters are required for the calculation of UVAI. In the future, we intend to

ACPD
9, 13569–13592, 2009

combine aerosol absorptive properties inferred from UVAI with auxiliary information, e.g. AOT and/or aerosol layer altitude from SCIAMACHY (reflectances in the visible, absorptions, or Raman scattering effects) or from other satellite instruments, in order to calculate aerosol radiative effects.

We plan to calculate UVAI from data from other satellite instruments such as GOME-2 and OMI. These instruments achieve global coverage nearly daily, and consequently provide us with better statistics. We will also use the aerosol information from UVAI to improve trace gas retrievals.

Acknowledgements. U. Platt, U. Pöschl, M. O. Andreae, A. Kokhanovsky, and P. Stammes are thanked for helpful discussions. IUP Bremen, A. Rozanov and V. Rozanov are kindly thanked for providing a pre-release version of SCIATRAN 3.0 (from http://www.iup.physik.uni-bremen.de/sciatran/downloads/), and for their excellent technical support. We would like to thank the ESA (European Space Agency) and the DLR (Deutsches Zentrum für Luft- und Raumfahrt) for providing us with the L1b SCIAMACHY data files. The US Geological Survey is acknowledged for making their topological data accessible (at http://edc.usgs.gov/products/elevation/gtopo30/gtopo30.html). We also thank the AERONET principal investigators B. Holben and R. Pinker and their staff for establishing and maintaining the GSFC, Walker Branch, Mongu and Ilorin sites. AERONET data were downloaded from: http://aeronet.gsfc.nasa.gov/.

M. P.d.V. acknowledges the Max Planck Society for a research grant.

The service charges for this open access publication
have been covered by the Max Planck Society.

References

Barnard, J. C., Volkamer, R., and Kassianov, E. I.: Estimation of the mass absorption cross section of the organic carbon component of aerosols in the Mexico City Metropolitan Area, Atmos. Chem. Phys., 8, 6665–6679, 2008, http://www.atmos-chem-phys.net/8/6665/2008/.

Bovensmann, H., Burrows, J. P., Buchwitz, M., Frerick, J., Noël, S., Rozanov, V. V., Chance,

K. V., and Goede, A. P. H.: SCIAMACHY: Mission objectives and measurements modes, J. Atmos. Sci., 56, 127–150, 1999.
Chand, D., Anderson, T. L., Wood, R., Charlson, R. J., Hu, Y., Liu, Z., and Vaughan, M.: Quantifying above-cloud aerosol using spaceborne lidar for improved understanding of cloudy-sky direct climate forcing, J. Geophys. Res., 113, D13206, doi:10.1029/2007JD009433, 2008.
Chiapello, I., Prospero, J. M., Herman, J. R., and Hsu, N. C.: Detection of mineral dust over the North Atlantic Ocean and Africa with the Nimbus 7 TOMS, J. Geophys. Res., 104(D8), 9277–9291, 1999.
Darmenova, K., Sokolik, I. N., and Darmenov, A.: Characterization of east Asian dust outbreaks in the spring of 2001 using ground-based and satellite data, J. Geophys. Res., 110, D02204, doi:10.1029/2004JD004842, 2005.
de Graaf, M., Stammes, P., Torres, O., and Koelemeijer, R. B. A.: Absorbing Aerosol Index – Sensitivity analysis, application to GOME and comparison with TOMS, J. Geophys. Res., 110, D01202, doi:10.1029/2004JD005178, 2005.
de Graaf, M. and Stammes, P.: SCIAMACHY Absorbing Aerosol Index – calibration issues and global results from 2002–2004, Atmos. Chem. Phys., 5, 2385–2394, 2005b, http://www.atmos-chem-phys.net/5/2385/2005/.
de Graaf, M., Stammes, P., and Aben, E. A. A.: Analysis of reflectance spectra of UV-absorbing aerosol scenes measured by SCIAMACHY, J. Geophys. Res., 112, D02206, doi:10.1029/2006JD007249, 2007.
Deutschmann, T.: Diploma Thesis, University of Heidelberg, 2008.
Dubovik, O., Holben, B., Eck, T. F., Smirnov, A., Kaufman, Y. J., King, M. D., Tanré, D., and Slutsker, I.: Variability of absorption and optical properties of key aerosol types observed in worldwide locations, J. Atmos. Sci., 59, 590–608, 2002.
Fromm, M., Bevilacqua, R., Servanckx, R., Rosen, J., Thayer, J. P., Herman, J., and Larko, D.: Pyro-cumulonimbus injection of smoke to the stratosphere: Observations and impact of a super blowup in northwestern Canada on 3–4 August 1998, J. Geophys. Res., 110, D08205, doi:10.1029/2004JD005350, 2005.
Fromm, M., Tupper, A., Rosenfeld, D., Servanckx, R., and McRae, R.: Violent pyro-convective storm devastates Australia's capital and pollutes the stratosphere, Geophys. Res. Lett., 33, L05815, doi:10.1029/2005GL025161, 2006.
Gleason, J. F., Hsu, N. C., and Torres, O.: Biomass burning smoke measured using backscattered ultraviolet radiation: SCAR-B and Brazilian smoke interannual variability, J. Geophys.

Res., 103(D24), 31969–31978, 1998.
Goldstein, A. H., Koven, C. D., Heald, C. L., and Fung, I. Y.: Biogenic carbon and anthropogenic pollutants combine to form a cooling haze over the southeastern United States, Proc. Nat. Acad. Sci. 106, 8835–8840, doi:10.1073/PNAS.0904128106, 2009.
Grzegorski, M., Wenig, M., Platt, U., Stammes, P., Fournier, N., and Wagner, T.: The Heidelberg iterative cloud retrieval utilities (HICRU) and its application to GOME data, Atmos. Chem. Phys., 6, 4461–4476, 2006, http://www.atmos-chem-phys.net/6/4461/2006/.
Herman, J. R., Bhartia, P. K., Torres, O., Hsu, C., Seftor, C., and Celarier, E.: Global distribution of UV-absorbing aerosols from Nimbus 7/TOMS data, J. Geophys. Res., 102(D14), 16911–16922, 1997.
Holben, B. N., Eck, T. F., Slutsker, I., Tanré, D., Buis, J. P., Setzer, A., Vermote, E., Raegan, J. A., Kaufman, Y. J., Nakajima, T., Lavenu, F., Jankowiak, I., and Smirnov, A.: AERONET – A federated instrument network and data archive for aerosol characterization, Remote Sens. Environ., 66, 1–16, 1998.
Hsu, N. C., Herman, J. R., Bhartia, P. K., Seftor, C. J., Torres, O., Thompson, A. M., Gleason, J. F., Eck, T. F., and Holben, B. N.: Detection of biomass burning smoke from TOMS measurements, Geophys. Res. Lett., 23(7), 745–748, 1996.
Hsu, N., Herman, J., Torres, O., Holben, B., Tanre, D., Eck, T., Smirnov, A., Chatenet, B., and Lavenu, F.: Comparisons of the TOMS aerosol index with Sun-photometer aerosol optical thickness: Results and applications, J. Geophys. Res., 104(D6), 6269–6279, 1999.
Hsu, N. C., Herman, J. R., and Tsay, S.-C.: Radiative impacts from biomass burning in the presence of clouds during boreal spring in southeast Asia, Geophys. Res. Lett., 30, 1224, doi:10.1029/2002GL016485, 2003.
Kirchstetter, T. W., Novakov, T., and Hobbs, P. V.: Evidence that the spectral dependence of light absorption by aerosols is affected by organic carbon, J. Geophys. Res., 109, D21208, doi:10.1029/2004JD004999, 2004.
Koelemeijer, R. B. A., Stammes, P., Hovenier, J. W., de Haan, J. F.: A fast method for retrieval of cloud parameters using oxygen A band measurements from the Global Ozone Monitoring Experiment, J. Geophys. Res., 106, 3475–3490, 2001.
Mahowald, N. M. and Dufresne, J.-L.: Sensitivity of TOMS aerosol index to boundary layer height: Implications for detection of mineral aerosol sources, Geophys. Res. Lett., 31, L03103, doi:10.1029/2003GL018865, 2004.

Mishchenko, M. I., Lacis, A. A., and Travis, L. D.: Errors induced by the neglect of polarisation in radiance calculations for Rayleigh-scattering atmospheres, J. Quant. Spectrosc. Radiat. Transfer, 51(3), 491–510, 1994.

Platt, U.: Differential Optical Absorption Spectroscopy (DOAS), in: Air monitoring by spectrometric techniques, edited by: Sigrist, M., pp. 27–84, John Wiley, New York, 1994.

Rozanov, V. V., Buchwitz, M., Eichmann, K.-U., de Beek, R., and Burrows, J. P.: SCIATRAN – A new radiative transfer model for geophysical applications in the 240–2400 nm spectral region: the pseudo-spherical version, Adv. Space Res., 29(11), 1831–1835, 2002.

Rozanov, A., Rozanov, V., Buchwitz, M., Kokhanovsky, A., and Burrows, J. P.: SCIATRAN 2.0 – A new radiative transfer model for geophysical applications in the 175–2400 nm spectral region, Adv. Space Res., 36, 1015–1019, 2005.

Tilstra, L. G., de Graaf, M., Noël, S., Aben, I., and Stammes, P.: SCIAMACHY's Absorbing Aerosol Index and the consequences of instrument degradation, Proc. ACVE-3, 2007

Tilstra, L. G.: SCIAMACHY Absorbing Aerosol Index Algorithm Theoretical Basis Document, SRON-EOS-RP-08-023, 2008.

Torres, O., Bhartia, P. K., Herman, J. R., Ahmad, Z., and Gleason, J.: Derivation of aerosol properties from satellite measurements of backscattered ultraviolet radiation: Theoretical basis, J. Geophys. Res., 103(D14), 17099–17110, 1998.

Torres O., Tanskanen, A., Veihelmann, B., Ahn, C., Braak, R., Bhartia, P. K., Veefkind, P., and Levelt, P.: Aerosols and surface UV products from Ozone Monitoring Instrument observations: An overview, J. Geophys. Res., 112, D24S47, doi:10.1029/2007JD008809, 2007.

van Diedenhoven, B., Hasekamp, O. P., and Aben, I.: Surface pressure retrieval from SCIAMACHY measurements in the O_2 A Band: validation of the measurements and sensitivity on aerosols, Atmos. Chem. Phys., 5, 2109–2120, 2005, http://www.atmos-chem-phys.net/5/2109/2005/.

Wagner, T., Dix, B., v. Friedeburg, C., Friess, U., Sanghavi, S., Sinreich, R., and Platt, U.: MAX-DOAS O_4 measurements – A new technique to derive information on atmospheric aerosols, J. Geophys. Res., 109, D22205, doi:10.1029/2004JD004904, 2004.

Wagner, T., Beirle, S., Deutschmann, T., Eigemeier, E., Frankenberg, C., Grzegorski, M., Liu, C., Marbach, T., Platt, U., and Penning de Vries, M.: Monitoring of atmospheric trace gases, clouds, aerosols and surface properties from UV/vis/NIR satellite instruments, J. Opt. A: Pure Appl. Opt., 10, 104019, doi:10.1088/1464-4258/10/10/104019, 2008.

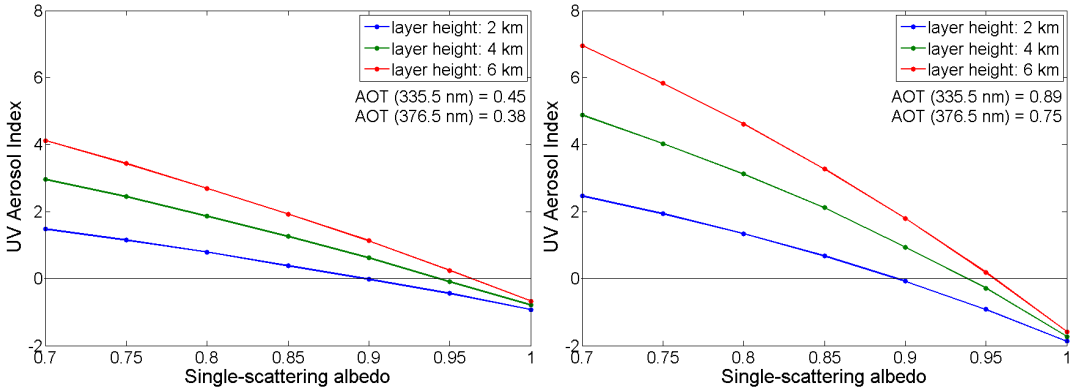

Fig. 1. Radiative transfer modelling (with SCIATRAN 3.0) of absorbing and scattering aerosols. UVAI were modelled for an aerosol layer as described in the text. Single-scattering albedo and layer height were varied, as indicated in the figure. The layer had total aerosol optical thickness of 0.45 and 0.38 (left figure) or 0.89 and 0.75 (right figure) at 335.5 and 376.5 nm, respectively, and a constant g-factor of 0.68. Calculations were performed for nadir viewing geometry and a solar zenith angle of 20°.

ACPD
9, 13569–13592, 2009

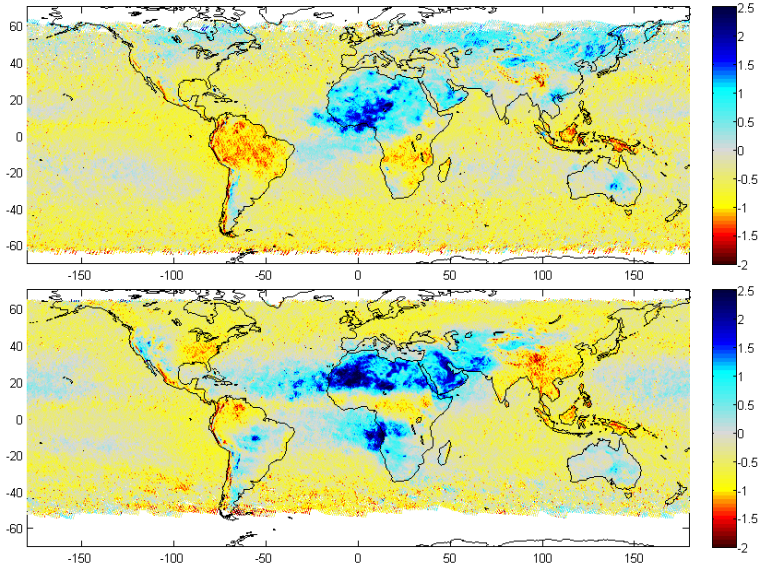

Fig. 2. Average UVAI for the months January, February, and March (upper figure) and July, August, and September (lower figure) 2005. Pixels with SZA >60° or in sun-glint geometry (see Sect. 2) were removed. The blue colour indicates the presence of absorbing aerosols, whereas the yellow-red colour indicates scattering aerosols and clouds.

ACPD

9, 13569–13592, 2009

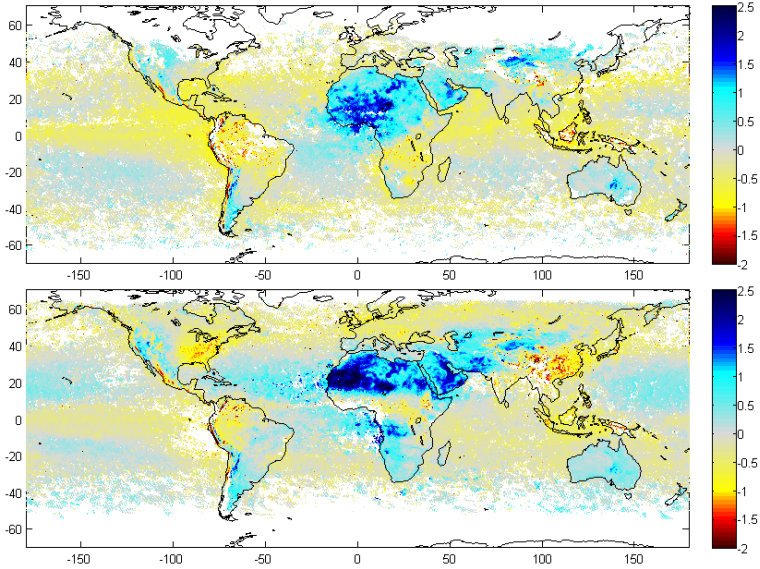

Fig. 3. Average UVAI for the months January, February, and March (upper figure) and July, August, and September (lower figure) 2005. Pixels with cloud fractions >5% (determined by the HICRU algorithm (Grzegorski et al., 2006)) were discarded, as were pixels with SZA >60° and those in sun-glint geometry (see Sect. 2). The blue colour indicates the presence of absorbing aerosols, whereas the yellow-red colour indicates scattering aerosols and clouds.

ACPD

9, 13569–13592, 2009

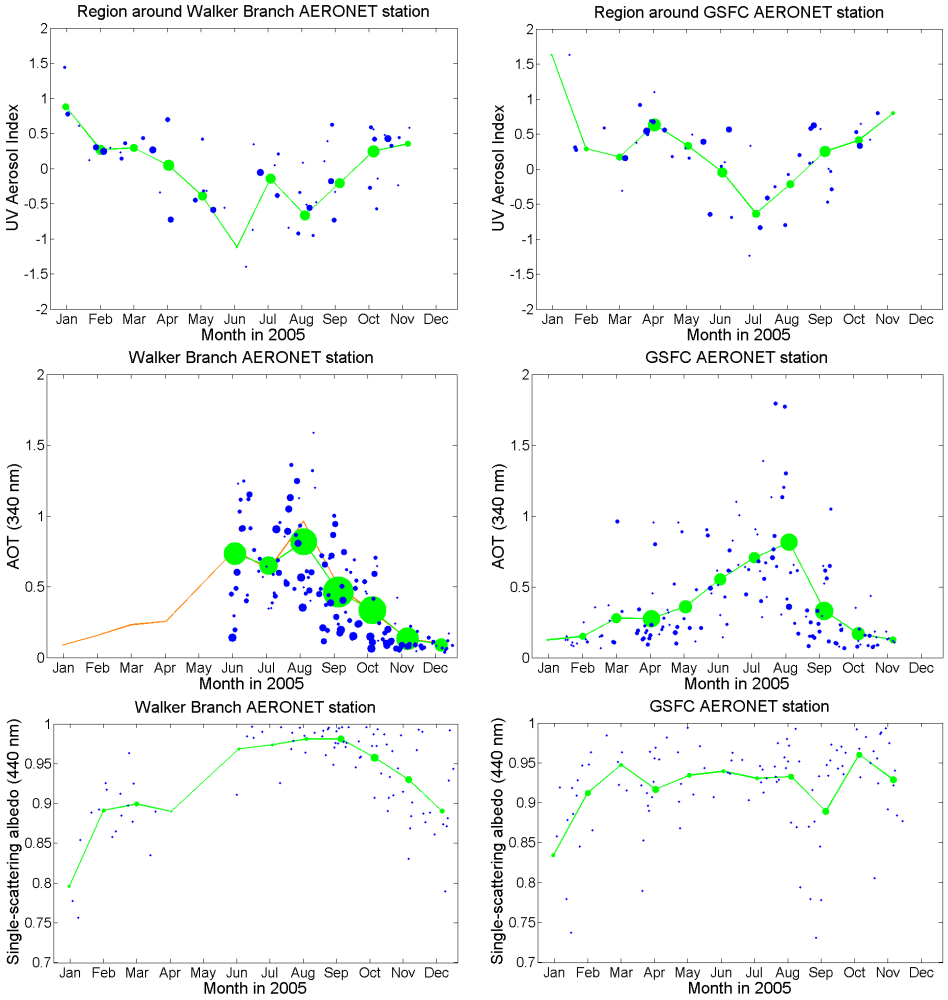

Fig. 4.

ACPD
9, 13569–13592, 2009

UV aerosol indices from SCIAMACHY

M. Penning de Vries et al.

Fig. 4. Time series of aerosol parameters at two AERONET stations in Southeast USA: left, Walker Branch (35° N, 84° W); right, GSFC (39° N, 77° W). Blue dots, daily averages; connected green dots, monthly averages. The size of the data points indicates the number of measurements included in the average value (minimum value: 1, maximum: 384 (monthly averaged AOT in October at Walker Branch).

Upper plots: daily and monthly averaged UVAI. Pixels included in the averaging were in a 2°×2° box with the AERONET station in the centre. Pixels with SZA >60° or with HICRU CF >5% were discarded.

Middle plots: AERONET AOT at 340 nm (level 2.0, only data for the orange line in the Walker Branch figure are level 1.5). Measurements included in the average have SZA <60°, and were measured between 9 and 11 a.m. (local time).

Lower plots: single-scattering albedo at 440 nm (level 1.5). The same criteria as for AOT measurements apply. Details are given in the text.

ACPD

9, 13569–13592, 2009

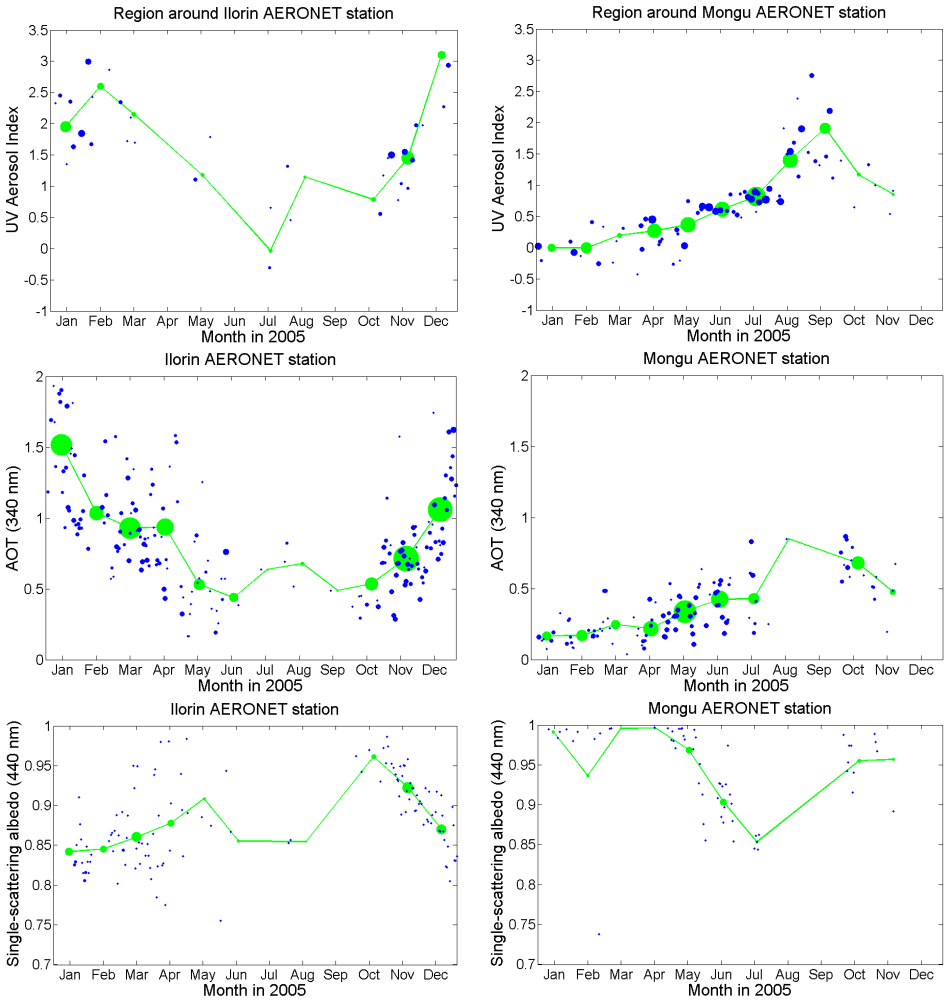

Fig. 5.

ACPD
9, 13569–13592, 2009

Fig. 5. Time series of aerosol parameters at two AERONET stations in Africa: left, Ilorin (8° N, 4° E); right, Mongu (15° S, 23° E). Blue dots, daily averages; connected green dots, monthly averages. The size of the data points indicates the number of measurements included in the average value (minimum value: 1, maximum: 264 (monthly averaged AOT in November at Ilorin)).

Upper plots: daily and monthly averaged UVAI. Pixels included in the averaging were in a 2°×2° box with the AERONET station in the centre. Pixels with SZA >60° or with HICRU CF >5% were discarded.

Middle plots: AERONET AOT at 340 nm (level 2.0). Measurements included in the average have SZA <60°, and were measured between 9 and 11 a.m. (local time).

Lower plots: single-scattering albedo at 440 nm (level 1.5). The same criteria as for AOT measurements apply. Details are given in the text.

ACPD
9, 13569–13592, 2009

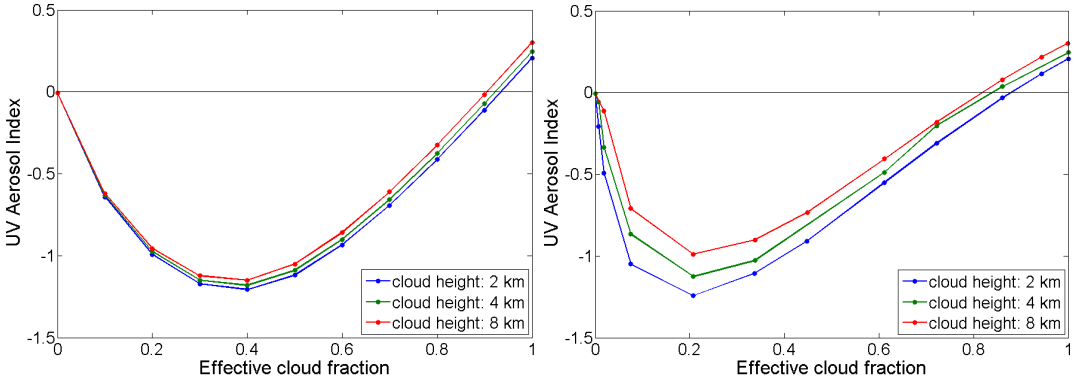

Fig. 6. Results from RTM calculations using SCIATRAN 3.0. Cloud parameters: single scattering albedo 1.0, asymmetry parameter 0.85. Left: thick clouds with a total cloud optical thickness equal to 50 (cloud albedo equal to 0.8) with varying geometrical cloud fraction. Right: clouds with varying cloud optical thickness (between 0.5 and 50) and geometrical cloud fraction equal to 1. Surface albedo was constant, and set to 0.05. Calculations were performed for nadir viewing geometry and a solar zenith angle of 20°.

ACPD
9, 13569–13592, 2009